J Mater Sci (2011) 46:5104–5110
DOI 10.1007/s10853-011-5440-9

Modeling the effect of reinforcement discontinuity on the tensile strength of UD flax fiber composites

J. Andersons · R. Joffe · E. Spārniņš · D. Weichert

Received: 12 January 2011 / Accepted: 3 March 2011 / Published online: 11 March 2011

Abstract To exploit the potential of natural fibers as reinforcement of polymer matrix composites, aligned bast fiber composite materials are being produced and studied. Bast fiber reinforcement is discontinuous due to the limited length of natural fibers, which needs to be reflected in predictive models of mechanical properties of composites. The strength in tension in the fiber direction of an aligned flax fiber-reinforced composite is modeled assuming that a cluster of adjacent fiber discontinuities is the origin of fracture. A probabilistic model of tensile strength, developed for UD composites containing a microdefect, is applied. It follows from the theoretical analysis that the experimental tensile strength as a function the fiber volume fraction can be described with acceptable accuracy assuming the presence of a cluster of ca. 4 × 4 elementary fiber discontinuities.

Introduction

Natural fiber composites with polymer matrices are being developed as an environmentally friendly alternative to traditional, man-made fiber-reinforced composites. In order to achieve the highest reinforcement efficiency, fibers need to be aligned [1]. For plant fibers traditionally used in textile industry, such as flax, alignment can be achieved e.g., by employing textile products such as rovings or yarns as the reinforcement [1–10] (while incurring additional cost associated to fiber spinning [11]). Although the rovings in the composite are straight and continuous, the natural fibers they are made of are somewhat misaligned owing to the twist of the roving, and discontinuous due to limited length of the fibers.

Bast fibers of flax used as reinforcement comprise elementary flax fibers and technical fibers that are bundles of naturally adhering elementary fibers. The average length of elementary flax fiber is ca. 3 cm and apparent diameter 19 μm [12]; the shape of its cross section is irregular, and the apparent diameter varies along a fiber as well as among fibers [13, 14]. Technical fiber length and diameter are also highly variable, being up to 75 cm [12] and 100 μm [15, 16] respectively, whereas the retained mutual adhesion of the elementary fibers forming a technical fiber is likely to be governed by the retting procedure employed.

Tensile strength of the elementary flax fibers at a fixed gauge length can be described by a two-parameter Weibull distribution [15, 17–19]. However, the variation of fiber strength with length was found to better comply with the modified Weibull distribution [20–22]

$$P(\sigma) = 1 - \exp\left[-\left(\frac{l}{l_0}\right)^{\alpha}\left(\frac{\sigma}{\sigma_0}\right)^{\rho}\right], \quad (1)$$

where ρ and σ_0 designate shape and scale parameters of the fiber batch strength distribution and α is a length exponent with values in the range of 0–1 (note that at $\alpha = 1$ Eq. 1 coincides with the Weibull two-parameter distribution).

Distribution function Eq. 1, originally proposed for fiber strength in [23, 24], has been interpreted in [25] to result from interfiber variability of strength distribution characteristics

J. Andersons (✉) · E. Spārniņš
Institute of Polymer Mechanics (IPM), University of Latvia, 23 Aizkraukles iela, Rīga LV-1006, Latvia
e-mail: janis.andersons@pmi.lv

R. Joffe
Division of Polymer Engineering, Luleå University of Technology (LTU), SE-971 87 Luleå, Sweden

D. Weichert
Institute of General Mechanics, RWTH-Aachen University, 52062 Aachen, Germany

of fibers in a batch. Specifically, it has been demonstrated by extensive numerical simulations that fiber batch strength distribution is closely approximated by Eq. 1 if each fiber in a batch possesses a two-parameter Weibull strength distribution

$$P_i(\sigma) = 1 - \exp\left[-\frac{l}{l_0}\left(\frac{\sigma}{\sigma_0^i}\right)^{\rho'}\right] \quad (2)$$

and all the individual fiber strength distributions have the same shape parameter, ρ', whereas the scale parameter σ_0^i varies randomly among fibers, having a distribution

$$P\left(\sigma_0^i\right) = 1 - \exp\left[-\left(\frac{\sigma_0^i}{\bar{\sigma}_0}\right)^{\mathrm{m}}\right]. \quad (3)$$

Relations for the distribution function Eq. 1 parameters in terms of those of Eqs. 2 and 3 have also been derived and reported in [25].

Fragmentation tests of elementary flax fibers confirmed that the strength distribution of individual fibers complies with the Weibull distribution, and the distribution parameters possess considerable scatter among fibers [20]. Moreover, correlation between the content of the largest mechanical damage entities of bast fibers, kink bands [15, 17, 26], in the flax fibers and the length exponent α values has been observed. Namely, little variability of node density between fibers is associated with α values in Eq. 1 approaching 1, while large variability leads to smaller α values [20, 22]. These findings lend support to the applicability of fiber strength model [25] to elementary flax fibers.

A probabilistic model of the tensile strength of a UD composite reinforced with continuous fibers possessing strength distribution Eq. 1 has been proposed in [25]. The model is an extension of the one developed for fibers with the Weibull two-parameter strength distribution [27]. It is based on the results of numerical simulations of the stochastic facture process by Monte Carlo method, employing 3D lattice Green's functions to account for the local load transfer from broken to intact fibers [27, 28]. However, the model is not directly applicable to flax fiber UD composites due to discontinuity and heterogeneity of the reinforcement.

Flax fiber aspect ratio is relatively large, therefore the reinforcing fibers can be considered as long. Fiber ends in an aligned short-fiber composite may serve as the starting points of cracks [29], particularly if several such discontinuities happen to be located adjacent to each other [30, 31]. The principal failure mechanism of a short-fiber-reinforced composite changes from fiber-avoiding crack propagation to a fiber-breaking mode already at relatively modest fiber aspect ratios [32, 33]. Hence, due to the large length-to-diameter ratio of flax fibers, a crack is likely to propagate by breaking of the fibers, and a probabilistic treatment of fracture process is needed to take into account the effect of fiber strength variability on the ultimate tensile strength of the composite material.

A cluster of adjacent discontinuities of fibers can be considered as a notch or a defect of the material. Probabilistic models of crack propagation from an initial defect in a UD composite in tension have been developed in [34–37] assuming Weibull distribution of fiber strength. The model [37] deals with the strength distribution of a composite containing a notch represented by a square cluster of nxn adjacent fiber breaks, located on a plane normal to the reinforcement direction. Approximate closed-form expressions have been derived for the parameters of the strength distribution, taking into account also the fiber pull-out effects.

Fiber discontinuities act as stress raisers in the flax fiber composite, therefore the likely failure location is expected to coincide with a cluster of adjacent fiber ends that would effectively act as a pre-crack. In order to make the strength analysis tractable, we model the complex disordered reinforcement morphology, shown schematically in Fig. 1a, by a regular array of completely separated elementary fibers, Fig. 1b, of the same fiber volume fraction. In this study, we apply the notch effect model [37], suitably modified for fiber strength distribution Eq. 1 as proposed in [25], to account for fiber discontinuity effect on the tensile strength of aligned flax fiber-reinforced composites.

Materials and methods

Flax fiber roving/vinyl ester matrix composites were produced and tested in tension as described in [10, 38, 39]. For completeness and convenience, we briefly recapitulate material characteristics, manufacture, and test procedure below.

Three types of roving, produced from ArcticFlax fibers, were employed. They were made of fine long line flax (roving N1), short flax fibers (roving N2), and two N2 rovings loosely, about 50 turn/m, twisted together (roving N3). The fibers were produced by FinFlax Oy (Finland) from flax harvested in the northern Finland and subjected to enzyme retting. The average apparent radius of fibers r_f amounted to 8 ± 2 μm [21]. Vinyl ester resin (Derakane 8090, Dow Chemicals) was used to impregnate the rovings. The following additives were applied per 100 g of resin: accelerator NL49-P (Akzo)—1 g; accelerator 9826 (Reichhold)—0.2 g; inhibitor 9853 (Reichhold)—0.2 g; initiator Trigonox 239—2 g.

Cylindrical specimens were manufactured via impregnation of roving, placed in a metal tube, by the resin. An in-house laboratory-scale resin transfer molding set-up was employed [38]. Upon post-curing of the specimens, end

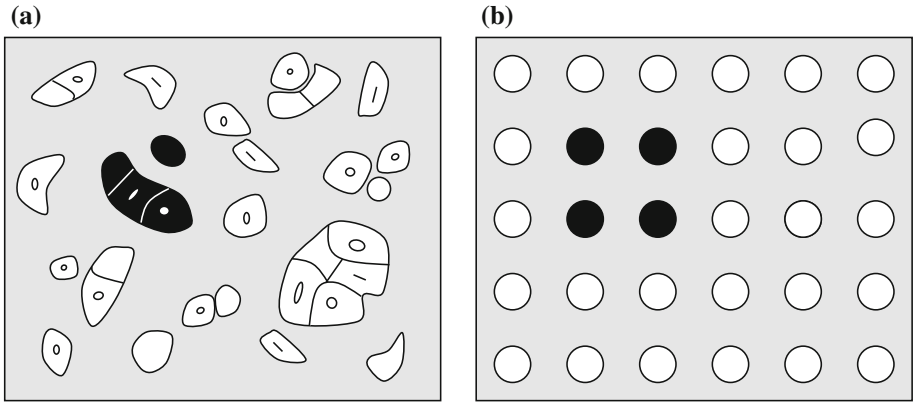

Fig. 1 Schematic of a cross section of UD flax fiber composite containing elementary and technical fibers (**a**) and an idealized model composite with regularly arranged elementary flax fibers of the same volume fraction (**b**). Discontinuous adjacent fibers forming a cluster are marked in *black*

tabs were molded and cured. The gauge length of the resulting dumb-bell shaped specimens was $L = 110$ mm and radius $R = 1.75$ mm within the gauge length. Specimens with fiber volume fraction $v_f = 0.17$ were produced from rovings of all three types, specimens with $v_f = 0.25$ from N3 roving and $v_f = 0.3$ from N1 roving. Micrographs of specimen cross sections, normal to the specimen axis, are shown in Fig. 2. Samples for microscopy were prepared by embedding pieces of impregnated bundles (3–4 bundles oriented vertically) into a soft polymer (Struers "EpoFix Resin") to form cylinders with the following dimensions: diameter $\approx$ 25 mm, height $\approx$ 20 mm. These specimens then were installed in a special holder (up to six samples per holder) and polished by using automatic Buehler polishing machine. At first, the specimens were ground with a grinding paper (240–1200 grit) to obtain flat surface and then polished by using disks with special surfaces and diamond liquids (with particle size down to 0.5 μm).

Tensile tests were carried out at LTU using Instron 4411 machine with 5 kN load cell on most of the specimens [10], while for tests of some specimens of N3 roving and $v_f = 0.25$, performed at IPM, Zwick/Roell electromechanical testing machine with 2.5 kN load cell was used [38]. The tests were performed under displacement control with loading rate of 2 mm/min. At least three specimens were tested within each batch. Stress was calculated from load and cross-section area of the bundle. The strength data obtained are shown in Fig. 3.

Model

Consider aligned discontinuous fiber-reinforced composite (Fig. 1b) under tension in the fiber direction. Since the strength of such a composite is determined by the maximum load taken by the fibers, statistical models of strength provide an estimate of the fiber stress σ_f, averaged over composite cross section, at failure of the composite. The strength of the composite is then given by $\sigma_c = \sigma_f v_f$ [40]. Should the matrix contribution be taken into account, the tensile strength of the composite can be evaluated as follows [25, 40]

$$\sigma_c = \sigma_f v_f + \sigma_m (1 - v_f), \tag{4}$$

where σ_m designate the stress carried by the matrix at the failure of the fibers in the composite material.

Denote the distribution function of σ_f by $P_0(\sigma_f)$ if the failure originates due to a breaking fiber, and by $P_i(\sigma_f)$ if the fracture takes place by crack propagation from a pre-existing discontinuity cluster comprising i fibers. Assuming that the random events of composite fracture by crack propagation from different locations are independent, the distribution function, $P_s(\sigma_f)$, of the critical fiber stress σ_f is expressed as

$$P_s(\sigma_f) = 1 - (1 - P_0(\sigma_f)) \prod_{i=1}^{l} (1 - P_i(\sigma_f))^{N(i)}, \tag{5}$$

where $N(i)$ is the number of fiber-end clusters of size i in the composite material, and l is the maximum cluster size.

Owing to elementary flax fibers being long with respect to the ineffective fiber length, the application of probabilistic models developed for continuous-fiber composites for evaluation of the probabilities in the RHS of Eq. 5 should lend results of acceptable accuracy. Then $P_0(\sigma_f)$ can be estimated by the model [25] as shown in [10] and $P_i(\sigma_f)$—by the model for square arrangement of fiber discontinuities described in [37]. Specifically, the probability of failure due to a fiber discontinuity cluster of size i is expressed as [37]

$$P_i(\sigma_f) = \Phi\left(\frac{\sigma_f - \left(\bar{\sigma}_c \frac{\mu^*}{K_i} + \sigma_p\right)}{\bar{\sigma}_c \frac{\gamma^{**}}{K_i}}\right) \tag{6}$$

with $\Phi(x)$ denoting the normal distribution function. Quantities μ^* and γ^{**} designating non-dimensional average and standard deviation of the strength of an intrinsic link (critical size fiber cluster) of an intact

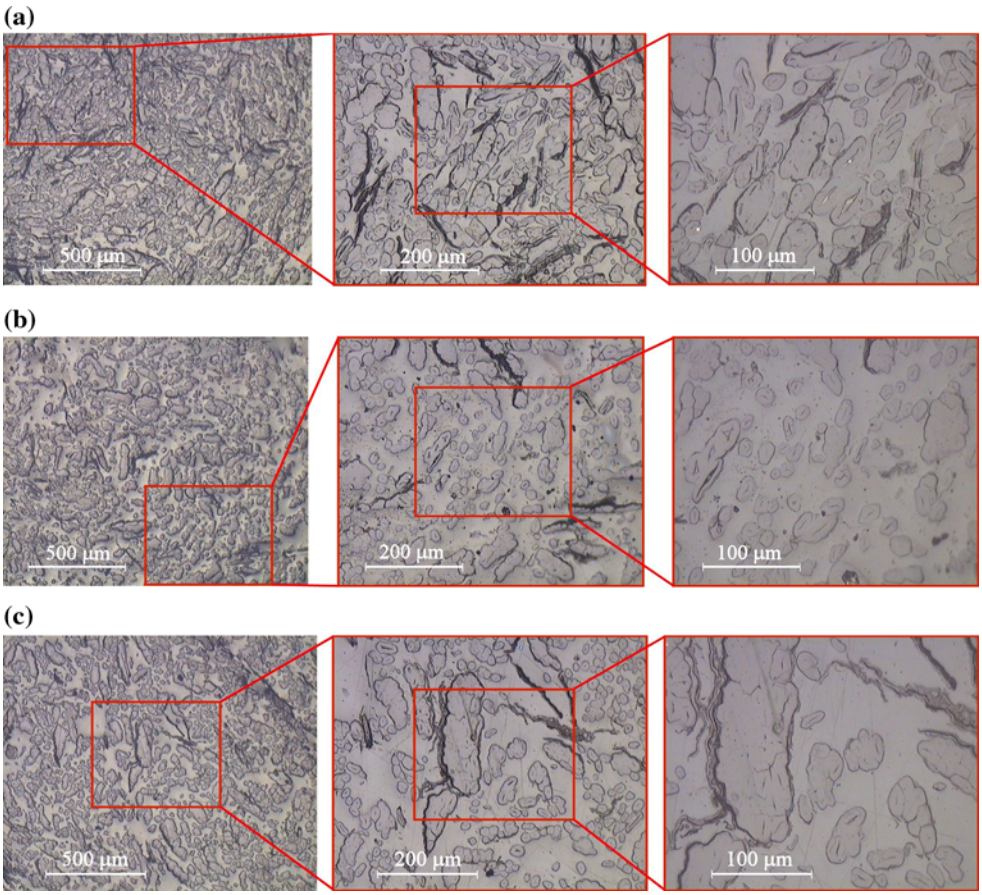

Fig. 2 Cross-section micrographs of impregnated roving N1 (**a**), N2 (**b**), and N3 (**c**)

composite have been presented as functions of the Weibull shape parameter ρ of fiber batch strength in e.g., [25]. Specifically, μ^* is approximated by the following relation

$$\mu^* = 0.6398 + 0.0238\rho - 0.0006\rho^2$$

valid for $2 \leq \rho \leq 10$. K_i in Eq. 6 is the stress concentration factor due to fiber discontinuity of size i [37], and $\bar{\sigma}_c$ is the characteristic stress defined via individual fiber Weibull shape parameter as suggested in [25]

$$\bar{\sigma}_c = \left(\frac{\tau l_0}{r_f}\right)^{\frac{1}{1+\rho'}} \bar{\sigma}_0^{\frac{\rho'}{1+\rho'}}. \tag{7}$$

The interfacial shear strength (IFSS) of the fiber and matrix is denoted by τ in Eq. 7, whereas ρ' and $\bar{\sigma}_0$ are parameters of the distribution functions Eqs. 2 and 3. The fiber pull-out stress σ_p in Eq. 6, based on the analysis of [41], is given by

$$\sigma_p = \bar{\sigma}_c \left(\frac{1}{1+\rho'}\right)^{\frac{\rho'}{1+\rho'}} \Gamma\left(\frac{2+\rho'}{1+\rho'}\right), \tag{8}$$

where Weibull shape parameter ρ' is used for consistency [25].

It has been demonstrated by numerical simulations in [37] that, should the initial defect be relatively large, the fracture process concentrates predominantly at it. Based on this finding, we assume that the strength of discontinuous-fiber composite is governed by the largest cluster of fiber breaks. Then the average fiber stress at the failure of composite is as follows from Eq. 6,

$$\langle \sigma_f \rangle = \bar{\sigma}_c \frac{\mu^*}{K_l} + \sigma_p, \tag{9}$$

where K_l is the maximum stress concentration factor at the largest discontinuity cluster [37].

Results and discussion

The theoretical relation for the tensile strength of a UD composite is obtained by substituting Eq. 9 into Eq. 4. However, it should be noted that the fiber pull-out stress expression, Eq. 8, is derived for regular-shape, cylindrical fibers that are subjected to constant interfacial shear stress during the pull-out process. Although the principal mechanism of apparent adhesion between flax fibers and

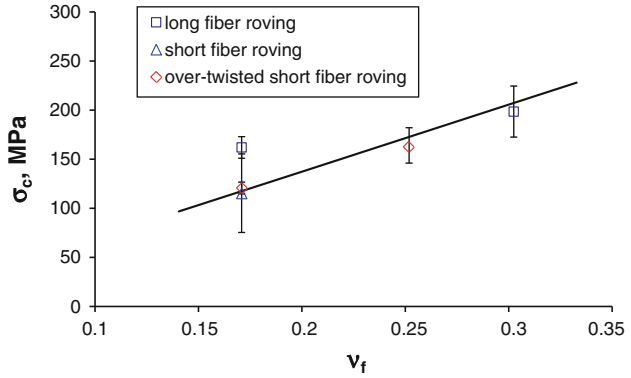

Fig. 3 Tensile strength of UD flax fiber composite as a function of fiber volume fraction. *Line* Eq. 10 for a cluster of 4 × 4 adjacent fiber discontinuities

polymer matrix is, arguably, friction and mechanical interlocking [42, 43], the pronounced variability of the apparent diameter along a flax fiber [13] is likely to result in significantly lower σ_p than that predicted by Eq. 8. Also, for fiber volume fractions of practical interest, the effect of the matrix strength term in Eq. 4 is minor. Therefore, as a first approximation, we neglect the contribution of fiber pull-out stresses and matrix stress at failure to the composite strength, and finally arrive at the relation

$$\sigma_c = v_f \bar{\sigma}_c \frac{\mu^*}{K_l}. \tag{10}$$

In order to apply Eq. 10 for tensile strength evaluation of a UD composite material, distribution parameters of Eqs. 1–3, interfacial shear strength and discontinuity cluster size have to be determined. The parameters of the elementary ArcticFlax fiber strength distribution, Eq. 1, are given in [20]. Those of Eqs. 2 and 3 can be easily calculated based on Eq. 1 using the analytical relations presented in [25]. The IFSS for ArcticFlax fibers and vinyl ester resin has been estimated at 16.8 MPa based on the pull-out length distribution of elementary fibers as observed on the fracture surfaces of impregnated bundles [38].

The theoretical average strength according to Eq. 10 has been compared with the test results for several K_l values corresponding to square arrangement of fiber discontinuities. The size of the *nxn* defect was selected so that the theoretical strength estimate provided best fit to the experimental data. It is seen in Fig. 3 that the presence of a cluster of 4 × 4 adjacent fiber discontinuities, with $K_{16} = 1.582$ [37], in the composite is consistent with the experimental strength data. Noting that a technical fiber contains up to tens of elementary fibers (see also Fig. 2), discontinuity of such a size could be generated by e.g., an abrupt termination of a single technical fiber. Direct verification of the presence and size of fiber discontinuity clusters in flax fiber composite, for example by microtomography, would allow more accurate description of the defect statistics in the composite, and hence application of more elaborate models, e.g., Eq. 5, reflecting the effect of the stochastic nature of defects on composite strength.

Fiber discontinuity distribution is likely to be a characteristic of fiber variety and pre-processing procedure. Then different composites produced from fibers of the same variety, pre-processed by the same method, should have comparable maximum discontinuity cluster size. Tensile strength of another UD ArcticFlax composite [44], produced by RTM of epoxy resin from a mat, obtained by combing and sewing flax fibers, is shown in Fig. 4 together with the prediction according to Eq. 10. The same fiber strength characteristics and discontinuity size as above, and IFSS estimate of fiber/epoxy interface $\tau = 33$ MPa obtained by fiber fragmentation test [45] were used in Eq. 10. It is seen in Fig. 4 that the predicted dependence of composite strength on fiber volume fraction is reasonably close to the test results.

The model presented neglects such characteristic features of quasi-UD bast fiber composites as fiber misalignment, disorder in fiber spacing, porosity, and fiber heterogeneity, that may affect to various extent the failure process and hence the strength of the composite material. Accounting for them would certainly enhance the predictive capacity of a composite strength model, although possibly necessitating involvement of heavily numerical simulation procedures.

The values of the maximum stress concentration factor K_l for different defect sizes evaluated and applied in [37] coincide with the classical results [46] obtained by shear-lag method. The latter is insensitive to the actual shape of fiber cross section since fiber stiffness is characterized by the product of its Young's modulus and cross-sectional area [40]. Therefore, at least in a shear-lag approximation, the K_l values derived for circular fibers are applicable also to flax fiber reinforcement with irregular-shape cross sections.

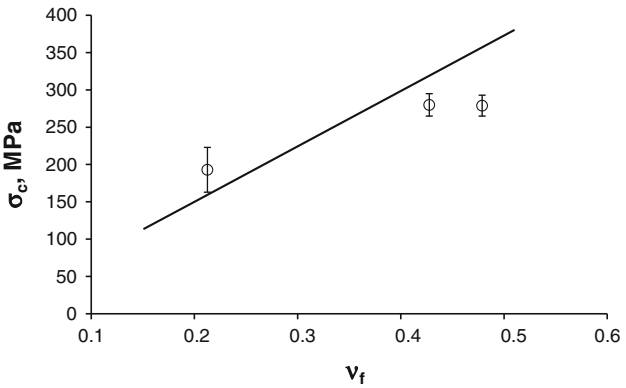

Fig. 4 Tensile strength of UD flax fiber composite as a function of fiber volume fraction [44]. *Line* Eq. 10 for a cluster of 4 × 4 adjacent fiber discontinuities

Disorder in fiber spacing and orientation is observed in both natural fiber and man-made continuous-fiber composites. Nominally unidirectional reinforcement by bundles of man-made continuous fibers has been shown to actually involve sizable fluctuations of local fiber volume fraction and fiber misorientation, particularly at bundle boundaries [47]. Considerable amount of experimental information regarding the actual, stochastic fiber arrangement has been accumulated, see e.g., [47–49]. Morphological disorder in UD composites affects their fracture via interfacial stress concentration in intact composites [50, 51] and by an increase in the overload experienced by an intact fiber closest to the broken one [52], thus facilitating premature fracture. These effects, however, are likely to be overshadowed in bast fiber composite by the stress concentration at a sizable cluster of fiber discontinuities considered above.

The peculiar geometry and morphology of the bast fibers and sub-optimal compatibilization with polymer matrices may lead to a relatively high void content in composites. Being markedly detrimental for the strength and stiffness of misoriented fiber composites (e.g., hemp/polyester [53]), the voids, however, are present in lower content and have a limited effect on the tensile strength of UD flax/polypropylene composites [3] (see also Fig. 2). Moreover, several semi-empirical relations for description of the reduction of strength due to voids have been considered, see e.g., [3, 54–57]. One of them has been applied to UD flax [3] and hemp [56] composite tension test results. Hence, such relations can also be incorporated in mechanistic strength models to approximately take into account the void effect.

A distinct feature of bast fiber composites is heterogeneity of the reinforcement, consisting of elementary and technical fibers, the latter exhibiting large scatter of geometrical dimensions. Technical flax fibers possess lower average tensile strength than elementary flax fibers and somewhat higher or comparable strength scatter at the same length, as evaluated by single fiber tension tests [15, 16]. If these fiber fracture characteristics are retained in a composite material, i.e., for fibers embedded in a polymer matrix, then technical fibers are likely to suffer the first breaks in the composite material. Therefore, further study of the fracture process of embedded technical fibers and its effect on composite strength appears warranted.

Conclusions

A statistical model of the tensile strength of an aligned flax fiber-reinforced polymer matrix composite has been developed, taking into account the presence in the composite of clusters of adjacent fiber discontinuities, treated as notches. The model has been applied to the strength data of ArcticFlax/polymer matrix composites, assuming that only the largest discontinuity cluster governs fracture of the composite. It was found that the presence of a 4×4 adjacent fiber discontinuities yields good agreement of the theoretical average strength with the test results.

Acknowledgements E. Spārniņš and J. Andersons acknowledge funding by ESF via project 2009/0209/1DP/1.1.1.2.0/09/APIA/VIAA/114. J. Andersons gratefully acknowledges the support by the DAAD which provided the opportunity for a research stay at the Institute of General Mechanics of the RWTH Aachen University. Authors are thankful to Mr. Alann Andre for help with manufacturing of samples and experimental work.

References

1. Hill C, Hughes M (2010) J Biobased Mater Bioenergy 4:148
2. Gassan J, Mildner I, Bledzki AK (1999) Mech Compos Mater 35:435
3. Madsen B, Lilholt H (2003) Compos Sci Technol 63:1265
4. Chabba S, Netravali AN (2004) JSME Int J Ser A 47:556
5. Chabba S, Netravali AN (2005) J Mater Sci 40:6275. doi: 10.1007/s10853-005-3143-9
6. Angelov I, Wiedmer S, Evstatiev M, Friedrich K, Mennig G (2007) Compos A 38:1431
7. Van de Weyenberg I, Chi Truong T, Vangrimde B, Verpoest I (2006) Compos A 37:1368
8. Goutianos S, Peijs T, Nystrom B, Skrifvars M (2006) Appl Compos Mater 13:199
9. Zhang L, Miao M (2010) Compos Sci Technol 70:130
10. Andersons J, Joffe R (2010) Compos A (submitted)
11. Dissanayake NPJ, Summerscales J, Grove SM, Singh MM (2009) J Biobased Mater Bioenergy 3:245
12. Lilholt H, Lawther JM (2000) In: Kelly A, Zweben C (eds) Comprehensive composite materials, vol 1. Pergamon Press, New York, p 303
13. Charlet K, Jernot JP, Eve S, Gomina M, Bréard J (2010) Carbohydr Polym 82:54
14. Charlet K, Jernot JP, Bréard J, Gomina M (2010) Ind Crops Prod 32:220
15. Bos HL, van den Oever MJA, Peters OCJJ (2002) J Mater Sci 37:1683. doi:10.1023/A:1014925621252
16. Romhány G, Karger-Kocsis J, Czigány T (2003) J Appl Poly Sci 90:3638
17. Davies GC, Bruce DM (1998) Textile Res J 68:623
18. Zafeiropoulos NE, Baillie CA (2007) Compos A 38:629
19. Andersons J, Spārniņš E, Joffe R (2009) J Mater Sci 44:685. doi: 10.1007/s10853-008-3171-3
20. Andersons J, Spārniņš E, Joffe R, Wallström L (2005) Compos Sci Technol 65:693
21. Andersons J, Poriķe E, Spārniņš E (2009) Compos Sci Technol 69:2152
22. Andersons J, Spārniņš E, Poriķe E (2009) J Compos Mater 43:2653
23. Gutans JA, Tamuzh VP (1984) Mech Compos Mater 21:1107 (in Russian)
24. Watson AS, Smith RL (1985) J Mater Sci 20:3260. doi: 10.1007/BF00545193
25. Curtin WA (2000) J Compos Mater 34:1301
26. Thygesen LG, Eder M, Burgert I (2007) J Mater Sci 42:558. doi: 10.1007/s10853-006-1113-5
27. Zhou SJ, Curtin WA (1995) Acta Metall Mater 43:3093
28. Ibnabdeljalil M, Curtin WA (1997) Int J Solids Struct 34:2649

29. Huang H, Talreja R (2006) Compos Sci Technol 66:2743
30. Fukuda H, Chou T-W (1981) J Mater Sci 16:1088. doi: 10.1007/BF00542756
31. Hikami F, Chou T-W (1984) J Mater Sci 19:1805. doi: 10.1007/BF00550251
32. Nishikawa M, Okabe T, Takeda N (2009) Adv Compos Mater 18:77
33. Okabe T, Takeda N, Nishikawa M (2010) Int J Damage Mech 19:339
34. Zweben C (1971) J Mech Phys Solids 19:103
35. Beyerlein J, Phoenix SL (1997) Eng Fract Mech 57:241
36. Beyerlein J, Phoenix SL (1997) Eng Fract Mech 57:267
37. Ibnabdeljalil M, Curtin WA (1997) Acta Mater 45:3641
38. Andersons J, Spārniņš E, Joffe R (2010) J Compos Mater (submitted)
39. Andre A (2004) Project Report, Luleå University of Technology, p 71
40. Phoenix SL, Beyerlein IJ (2000) In: Kelly A, Zweben C (eds) Comprehensive composite materials, vol 1. Elsevier, Amsterdam, p 559
41. Thouless MD, Evans AG (1988) Acta Metall 36:517
42. Thomason JL (2009) In: Proceedings of ICCM-17, 27–31 July 2009, Edinburgh, UK
43. Thomason JL (2010) Polym Compos 31:1525
44. Oksman K (2001) J Reinf Plast Compos 20:621
45. Joffe R, Andersons J, Wallström L (2005) J Mater Sci 40:2721. doi:10.1007/s10853-005-2115-4
46. Hedgepeth JM, Van Dyke P (1967) J Compos Mater 1:294
47. Requena G, Fiedler G, Seiser B, Degischer P, di Michiel M, Buslaps T (2009) Compos A 40:152
48. Pyrz R (1994) Compos Sci Technol 50:197
49. Silberschmidt VV (2006) J Mater Sci 41:6768. doi: 10.1007/s10853-006-0205-6
50. Pyrz R, Bochenek B (1998) lnt J Solids Struct 35:2413
51. Kushch VI, Shmegera SV, Mishnaevsky L (2009) J Mech Mater Struct 4:1089
52. Landis CM, McMeeking RM (1999) Int J Solids Struct 36:4333
53. Patel HK, Ren G, Hogg PJ, Peijs T (2010) Plast Rubber Compos 39:268
54. de Almeida SFM, Neto ZSN (1994) Compos Struct 28:139
55. Liu L, Zhang B, Wu Z, Wang D (2005) J Mater Sci Technol 21:87
56. Madsen B, Hoffmeyer P, Lilholt H (2007) Compos A 38:2204
57. Guo Z-S, Liu L, Zhang B-M, Du S (2009) J Compos Mater 43:1775